

Polyaniline-TiO₂/graphene nanocomposite: an efficient catalyst for the removal of anionic dyes

Robab Mohammadi*, Bakhshali Massoumi, Fariba Galandar

Department of Chemistry, Payame Noor University, P.O. Box 19395-3697, Tehran, Iran, Tel. +98 41 35421414; Fax: +98 41 35431067; email: mohammadi_rb@yahoo.com (R. Mohammadi), Tel. +98 41 35492303; Fax: +98 41 35412108; email: b_massoumi@pnu.ac.ir (B. Massoumi), Tel. +98 41 35412117; Fax: +98 41 35419221; email: faribagalandar72@gmail.com (F. Galandar)

Received 14 June 2018; Accepted 24 November

ABSTRACT

In this work, titanium dioxide (TiO₂), TiO₂/graphene (TiO₂/GO) and polyaniline-TiO₂/graphene (polyaniline-TiO₂/GO) catalysts were prepared and characterized by different analysis methods such as X-ray diffractometer, transmission electron microscope, scanning electron microscope, energy-dispersive X-ray spectroscopy, Brunauer–Emmett–Teller and diffuse reflectance spectra. The photocatalytic activity and adsorption capacity of prepared samples were investigated by the removal of methyl orange as an anionic dye from aqueous solutions. Polyaniline-TiO₂/GO nanocomposite presented high photocatalytic activity, which is partly due to the sensitizing effect of polyaniline and the low recombination rate due to the graphene oxide electron scavenging property. In order to study the nature of adsorption procedure, the equilibrium adsorption isotherms were investigated. The linear correlation coefficients of Langmuir and Freundlich isotherms were obtained. Based on results, Langmuir isotherm model fitted the experimental data better than Freundlich isotherm model. According to the Langmuir isotherm model, the maximum adsorption capacity of Polyaniline-TiO₂/GO nanocomposite for sequestering methyl orange was about 69.23 mg g⁻¹. Furthermore, negative free energy change (ΔG°) and enthalpy change (ΔH°) values resulted from thermodynamic investigation suggested that the adsorption of methyl orange onto polyaniline-TiO₂/GO nanocomposite was spontaneous and exothermic in nature, respectively.

Keywords: Polyaniline-TiO₂/GO nanocomposite; Anionic dye; Photocatalytic activity; Adsorption procedure; Thermodynamic investigation

1. Introduction

Methyl orange is a well-known acidic/anionic dye and has been widely applied for different applications such as textiles, papers, plastics, printing, cosmetics and mineral processing [1]. Because of the synthetic origin and complex aromatic molecular structure, methyl orange is resistant to biodegradation and very stable to light and oxidation [2]. Also, this type of dye is toxic and mutagenic to different forms of life and can cause a significant impact on human health because of its mutagenic and carcinogenic influences [3]. So, the removal of this noxious dye from aqueous environment is necessary. In

recent years, remarkable efforts such as biological treatment [4], chemical oxidation [5], membrane separation [6] and adsorption [7] have been performed to remove dyes from wastewater. Among all these methods, adsorption technique is regarded as a highly efficient and economical method to produce water with high quality. In adsorption procedure, elimination of contaminant pollutant from wastewater is conducted via binding it to an adsorbent [8]. The binding can be done by ion exchange, electrostatic, Vander Waals, etc. The application of nano-adsorbents in adsorption of pollutants from wastewater, because of their high surface area to volume ratio, remarkable adsorption and desorption capacity and high reactivity, has gained impetus in recent years [9]. Various nano-adsorbents, including TiO₂/graphene-alginate

* Corresponding author.

nanocomposite [10], carbon nanotubes-encapsulated barium cross-linked alginate beads [11], copper oxide nanoparticle loaded on activated carbon (Cu₂O-NP-AC) [12], magnetic oxidized multi-walled carbon nanotube-k-carrageenan-Fe₃O₄ nanocomposite [13] and silica/chitosan nanocomposite [14], have been applied for the removal of pollutants from wastewater. Adsorption technique is an appropriate and economic way to produce water with high quality. In adsorption process, elimination of pollutant from wastewater is conducted via binding it to an organic or inorganic adsorbent. The binding can be done by ion exchange, electrostatic, Van der Waals, etc. TiO₂ is one of the most investigated semiconductors owing to excellent electronic properties, non-toxicity, cheapness, capability of repeated use without substantial loss of catalytic ability and high reactivity [15]. However, TiO₂ has low photo quantum efficiency because of its fast recombination of photogenerated electron-hole pairs [16]. In order to solve the above problem and modify the electronic structure of TiO₂, considerable efforts have been directed to enhance the photocatalytic efficiency and visible-light utilization of TiO₂ which include impurity doping, sensitization and metallization, etc. Among these methods, sensitization with conducting polymers has been proved to be an effective technique to improve the photocatalytic efficiency of TiO₂-based photocatalysts [17]. Among different conducting polymers, polyaniline is unique because of its facile synthesis, environmental and chemical stability and simple doping/dedoping chemistry [18]. Polyaniline can absorb light and induce a $\pi-\pi^*$ transition and the excited electrons can be transferred to the π^* orbital and the excited electrons are injected readily into the conduction band (CB) of TiO₂ which lowers the band gap of TiO₂. Therefore, polyaniline acts as sensitizer of TiO₂ via decreasing its band gap [19].

In recent years, graphene has received research interest because of its thermal and chemical stability, large surface-to-volume ratio, good electron conductivity and water solubility [20]. One of the most important characteristics of graphene is its large theoretical specific surface area, which makes it an excellent candidate for the use as an adsorbent material. Therefore, graphene because of its high conductivity and mobility can act as an electron scavenger which can reduce the recombination rate [21]. So, it is believed that a nanocomposite of graphene/TiO₂ with polyaniline will exhibit enhanced photocatalytic activity because of the low band gap, low recombination rate and high absorption under ultraviolet (UV) and visible region, due to the synergism between the constituents. The aim of the present study is to prepare polyaniline-TiO₂/GO nanocomposite and evaluate its photocatalytic activity and adsorption capacity for the removal of an anionic dye (methyl orange) in aqueous solutions. To the best of our knowledge, there is no report on the application of polyaniline-TiO₂/GO nanocomposite for the removal of anionic dyes such as methyl orange in aqueous solutions.

2. Materials and methods

2.1. Materials

Titanium n-butoxide, ethanol of absolute grade, graphite powder (purity 99.999%), nitric acid, sulfuric acid, potassium chlorate, hydrochloric acid, anisidine, ammonium

persulphate (APS) and methyl orange were purchased from Merck Co. (Germany). All chemicals were of AR grade and used as received except aniline which was distilled under reduced pressure and kept below 4°C before used for synthesis. Deionized water was used in all synthesis.

2.2. Sample preparation

2.2.1. Preparation of TiO₂ catalyst

TiO₂ nanoparticles was prepared by sol-gel method according to our previous work [16].

2.2.2. Preparation of graphene oxide sample

According to [10], graphene oxide was prepared via Staudenmaier method. First, 5 g graphite was mixed with concentrated nitric acid (45 mL) and sulfuric acid (90 mL) and stirred vigorously for 20 min to get dispersion. Next, potassium chlorate (55 g) was slowly added over 30 min, to avoid sudden increases in temperature, and the reaction mixture was stirred for 72 h at room temperature. The mixture was then added into a copious amount of distilled water and then filtered. The obtained graphite oxide solid was rinsed repeatedly and washed with a 5% solution of HCl and water repeatedly until the pH of the filtrate was neutral. The graphite oxide thus obtained was placed in a quartz boat and inserted into a tubular furnace preheated to 1,050°C and kept at this temperature for 30 s.

2.2.3. Preparation of TiO₂/GO sample

In our previous work, we reported preparation of TiO₂/GO catalyst via hydrothermal process [10]. Graphene oxide (20 mg) was dissolved in a solution of distilled water (80 mL) and ethanol (40 mL) via ultrasonic treatment for 2 h. TiO₂ (200 mg) was added to the synthesized graphene oxide solution and stirred for further 2 h to obtain a homogeneous suspension. The suspension was then placed in a 200 mL Teflon-sealed autoclave and maintained at 120°C for 3 h to simultaneously achieve the reduction of graphene oxide and the deposition of TiO₂ on the graphene sheets. Finally, the obtained sample was recovered via filtration, rinsed with high purity deionized water for several times and dried at 70°C for 12 h in the vacuum furnace.

2.2.4. Preparation of polyaniline-TiO₂/GO nanocomposite

Polyaniline-TiO₂/GO nanocomposites with various polyaniline contents were synthesized by chemical oxidative polymerization of aniline in the presence of TiO₂/GO particles. First, 2 mg of nanocrystalline TiO₂/GO particles were dispersed into 80 mL of 1 mol L⁻¹ HCl aqueous solutions with ultrasonic vibrations for 10 min to obtain a homogeneous suspension. Quantitative aniline was added into this mixture dropwise under vigorously stirring in the ice-water bath, after which APS was dissolved in 1 mol L⁻¹ HCl aqueous solutions with the molar ratio of aniline to APS (1:0.25) was added to the reaction vessel. Then, the mixture was allowed to polymerize under stirring for 2 h. Finally, polyaniline-TiO₂/GO nanocomposites were filtered and washed with large amount of deionized water, then with 80 mL of ethanol and 40 mL

of ether, after that the nanoparticles were dried at 80°C till the constant mass was reached. In the experiment, various initial weight ratios of aniline to TiO₂/GO (3%, 5%, 10%, 15% and 20%) were used to obtain the optimum content of aniline. The synthesized samples were designated as 3 polyaniline-TiO₂/GO, 5 polyaniline-TiO₂/GO, 10 polyaniline-TiO₂/GO, 15 polyaniline-TiO₂/GO and 20 polyaniline-TiO₂/GO respectively. Finally, the best catalyst procured in this method was designated as polyaniline-TiO₂/GO.

2.3. Characterization of prepared samples

To identify and confirm the crystal phase composition and the crystallite size of the products, X-ray diffractometer (XRD) analyses with XRD using Cu K α radiation (0.15478 nm) in the 2 θ scan range of 10°–70° were performed. For analysis, the (1 0 1) diffraction peak with 2 θ = 25.334° of anatase and (1 1 0) peak with 2 θ = 27.967° of rutile were used. The average crystallite size of the samples was calculated using Scherrer's formula [21]:

$$D = \frac{k\lambda}{\beta \cos\theta} \quad (1)$$

where D is the average crystallite size (Å), λ the wavelength of X-ray radiation (Cu K α), β the full width at half maximum (FWHM) intensity of the peak and θ the Bragg diffraction angle. The texture and morphology of products were observed on a Philips XL-30ESM scanning electron microscope (SEM) and a Philips CM-10 HT transmission electron microscope (TEM) with an accelerating voltage of 100 kV. The chemical composition of the synthesized nanocomposite was analyzed by an energy-dispersive X-ray spectroscopy (EDX) system. Brunauer–Emmett–Teller (BET) measurement was performed using Belsorp mini II instrument based on N₂ adsorption–desorption isotherms. Ultraviolet/visible diffuse reflectance spectra (DRS) of samples were performed by Avaspec-2048 TEC spectrometer in order to detect the band gap energy (E_g) of products which estimated via the following formula:

$$E_g = \frac{h \times c}{\lambda} = \frac{1,240}{\lambda} \quad (2)$$

where E_g is the band gap energy (eV), h is Planck's constant (4.1357×10^{-15} eV), c is the light velocity (2.998×10^8 m s⁻¹) and λ is the wavelength (nm).

2.4. Studies and analysis

The photocatalytic activity of prepared samples was evaluated in the removal of model compound methyl orange. The photocatalytic removal of methyl orange was measured at ambient pressure and room temperature in a batch quartz reactor, as previously reported [22]. Artificial illumination was provided by 36 W (UV-A) mercury lamp (Philips, Holland) with a wavelength peak at 365 nm positioned above the photoreactor. In each run, 400 mg L⁻¹ prepared sample and 20 mg L⁻¹ methyl orange were fed into the batch quartz reactor and placed in the dark condition for 30 min with continuous stirring for adsorption–desorption equilibrium and then exposed to black-light irradiation. The zero time

reading was obtained from blank solution kept in the dark. The photocatalytic reaction was then started via irradiating the suspension with black light. Every 4 min as interval time, 5 mL of the dye suspension was withdrawn and centrifuged to remove catalyst particles. The concentration of remaining methyl orange was determined by UV–Vis Perkin–Elmer 550 SE spectrophotometer at the wavelength of 465 nm. Experimental setup for the adsorption of methyl orange via polyaniline-TiO₂/GO nanocomposite was similar to that of the photocatalytic removal of methyl orange. However, for the batch adsorptive removal of methyl orange via polyaniline-TiO₂/GO nanocomposite without light illumination, the setup was placed inside a fully covered box in order to prevent any exposure toward light irradiation. The amount of methyl orange adsorbed onto polyaniline-TiO₂/GO nanocomposite was estimated by Eq. (3):

$$q = \frac{(C_0 - C)V}{M} \quad (3)$$

where q , C_0 and C are the amount of adsorbed methyl orange (mg g⁻¹), the initial concentration and the final concentration of dye in the solution (mg L⁻¹), respectively. In addition, V is the volume of the solution (L) and M is the weight of the nanocomposite (g) [23].

3. Results and discussion

3.1. Characterization of synthesized samples

3.1.1. X-ray diffraction

XRD patterns of TiO₂, TiO₂/GO and Polyaniline-TiO₂/GO samples are illustrated in Fig. 1. As shown in Fig. 1, the diffraction peaks of all samples were observed at 2 θ = 25.43°,

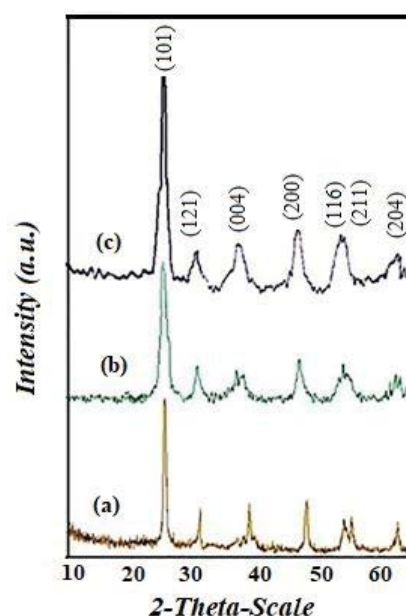


Fig. 1. XRD patterns of (a) TiO₂, (b) TiO₂/GO and (c) polyaniline-TiO₂/GO.

30.76°, 37.82°, 48.0°, 54.5° and 63.04° correspond to reflections (101), (121), (004), (200), (105)/(211), (204). The diffraction peaks can be assigned to mainly a mixture of anatase (TiO_2 , JCPDS card #84-1286) and brookite phases (TiO_2 , JCPDS card #72-0100). Pure anatase phase can be observed for synthesized samples. The crystallite size of samples is estimated via the Scherrer's formula based on the FWHM intensity of anatase (1 0 1) phase. The average size of crystallites for TiO_2 and TiO_2/GO determined from the XRD pattern based on the Scherrer's equation were about 14 and 12 nm, respectively. As can be seen in Fig. 1(b), the crystallinity of TiO_2/GO is higher than that of TiO_2 . In explanation, when TiO_2 nanoparticles are grown on the surface of the GO sheets, the functional groups on the GO sheets act as templates, enhancing crystallization and resulting in smaller sized TiO_2 nanoparticles being resulted [15]. Fig. 1(c) shows XRD patterns of polyaniline- TiO_2/GO nanocomposite. It can be seen that there is no difference between XRD pattern of polyaniline- TiO_2/GO nanocomposite and XRD pattern of other samples, which reveals deposition of polyaniline on the surface of TiO_2/GO has no influence on the crystallinity of TiO_2/GO . The average size of crystallites for polyaniline- TiO_2/GO nanocomposite determined from the XRD pattern based on the Scherrer's formula was 10 nm. Therefore, the mean size of TiO_2/GO is not affected via the polyaniline modification [24]. However, no typical diffraction peaks of GO or polyaniline are observed in the prepared samples. This can be explained via the fact that only small amounts of GO and polyaniline are contained in the synthesized samples [25].

3.1.2. SEM analysis of polyaniline- TiO_2/GO nanocomposite

SEM image was recorded to investigate the morphology and aggregation level of materials. Fig. 2 demonstrates SEM micrograph of polyaniline- TiO_2/GO nanocomposite. The morphology of prepared nanocomposite seems to be sphere. Interestingly, the pure polyaniline agglomerates were not detected in SEM micrograph, which agrees with conclusions that polyaniline in polyaniline- TiO_2/GO nanocomposite mainly covers the TiO_2/GO surface. As can be seen that, SEM image exhibits particles with good homogeneity, granular

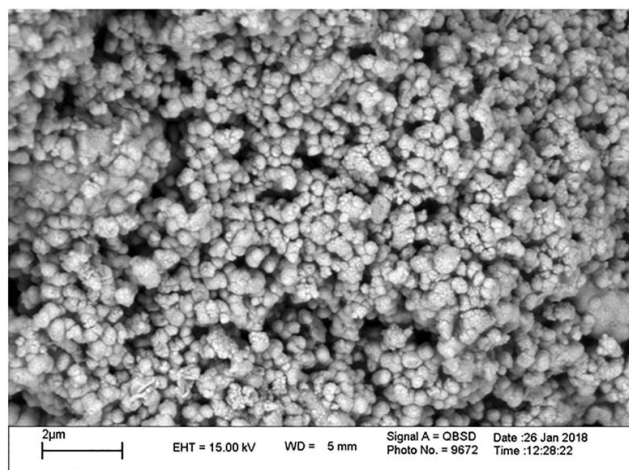


Fig. 2. SEM image of polyaniline- TiO_2/GO nanocomposite.

structure and slight agglomeration. Slight agglomeration may be due to the formation of polyaniline on the surface of TiO_2/GO nanoparticles which causes repulsion forces between nanoparticles and prevents their agglomeration. Since less particle agglomeration occurred for polyaniline- TiO_2/GO nanocomposite, the large surface area conveys high adsorption abilities of this sample. There are short slit-pores, which is in good agreement with the N_2 sorption isotherms results.

3.1.3. Elemental analysis with EDX spectroscopy

The elemental composition of the prepared nanocomposite was determined using EDX analysis. C, O, N and Ti peaks can be clearly seen from Fig. 3. EDX analysis showed no significant levels of impurities, which could have originated from the procedure.

3.1.4. TEM Analysis of Polyaniline- TiO_2/GO nanocomposite

TEM image of polyaniline- TiO_2/GO nanocomposite is shown in Fig. 4. The average size of the primary particles estimated from the TEM image is about 8–10 nm, which is in good agreement with that calculated from the XRD pattern using Scherrer equation. It can be observed that the particles show a relatively uniform particle size distribution. The degree of agglomeration can be avoided through the growth of TiO_2 nanoparticles from carboxyl groups on the surface of GO nanosheets [26]. Therefore, GO nanosheets can facilitate a uniform dispersion of the nanoparticles on its surface. As shown in TEM image, polyaniline layers on the TiO_2 surface attached together and generated the porous structure. This is a result of polymer growth on the surface of nanoparticles. Since composites made from metal oxide nanomaterials show considerable stability (owing to metal oxide nanomaterial structures), this approach is used for applied purposes [27]. The porous structure of polyaniline on the TiO_2 surface and elsewhere is an important characteristic that allows specific interactions of polyaniline- TiO_2/GO nanocomposite with methyl orange molecules, making it an important feature for the photocatalytic and adsorption performances [28].

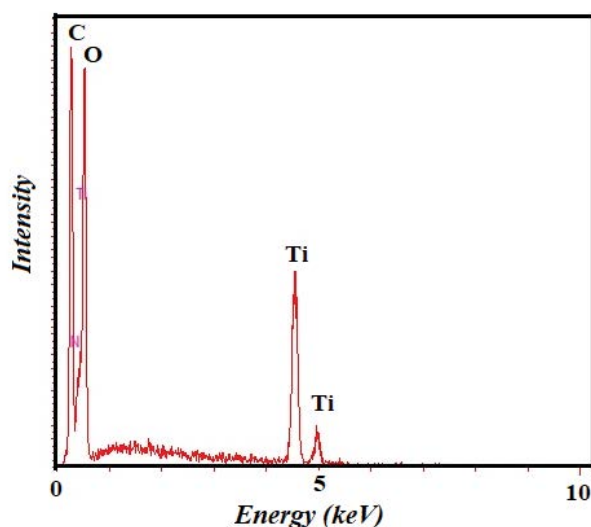


Fig. 3. EDX pattern of polyaniline- TiO_2/GO nanocomposite.

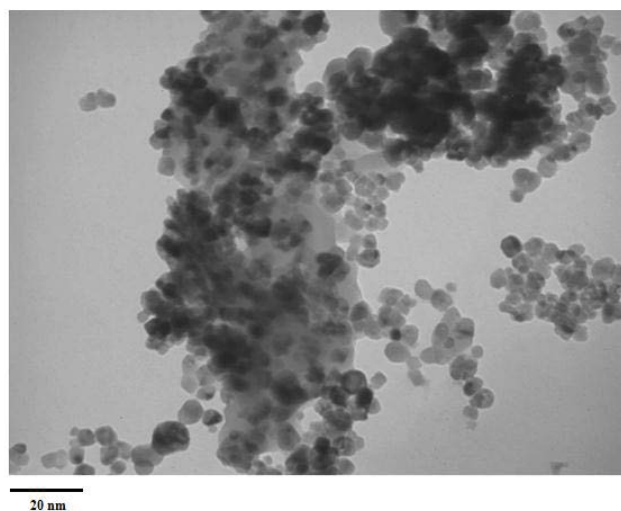


Fig. 4. TEM image of polyaniline-TiO₂/GO nanocomposite.

3.1.5. DRS analysis

In order to study the effect of graphene oxide and polyaniline on the optical absorption properties of TiO₂, DRS analysis has been carried out (Fig. 5). The reflectance spectra of TiO₂, and TiO₂/GO, show absorption thresholds at 390 and 410 nm, respectively, and E_g values estimated from the Eq. 3 are 3.17 and 3.02 eV, respectively. It can be concluded that graphene sheets narrow the band gap of TiO₂ [22]. These phenomenon results not only from the high conductivity of graphene that can facilitate separation of photogenerated e^-/h^+ pairs [21] but also from the formation of Ti–O–C bonding between TiO₂ and graphene sheets [13]. Furthermore, this may be related to the charge transfer between CB of TiO₂ and graphene sheets. However, the electron transition from the valence band to the CB can occur easier with the band-gap narrowing in TiO₂ nanoparticles [10]. The band gap energy (E_g) of polyaniline-TiO₂/GO is 2.81 eV. It can be concluded that polyaniline induces band-gap narrowing in TiO₂/GO catalyst. This may be attributed to the coordination of TiO₂ with the nitrogen atom, and a possible π – π interaction between GO and polyaniline via the pi-conjugated system. So, polyaniline-TiO₂/GO can be excited by absorbing both UV

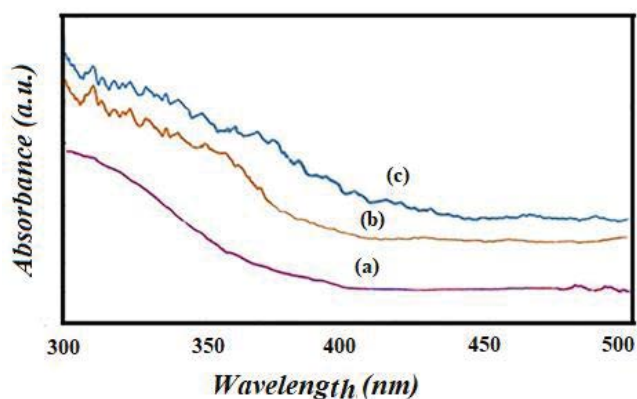


Fig. 5. UV–Vis DRS spectra of (a) TiO₂, (b) TiO₂/GO and (c) polyaniline-TiO₂/GO.

and visible lights to produce more electron–hole pairs and give a maximum visible light harvesting. As a consequence, polyaniline-TiO₂/GO composite is a promising material for the efficient use of light in photocatalytic procedures.

3.1.6. BET analysis

Fig. 6 shows the nitrogen adsorption–desorption isotherms of polyaniline-TiO₂/GO nanocomposite, which provide information about the structural properties and pore geometries of the synthesized sample. From this figure, polyaniline-TiO₂/GO nanocomposite exhibits a type IV adsorption isotherm according to the International Union of Pure and Applied Chemistry (IUPAC) classification related to mesoporous size (2–50 nm). Also, mesoporosity may be concluded from the sharp decline in the desorption branch and the hysteresis loop at high relative pressure. At high relative pressures from 0.55 to 0.85, the shape of hysteresis loop is of type H₂, indicating the existence of an ink bottle-type pores structure with narrow necks and wide bodies, implying that the crystallites contain mesopores due to the aggregation of particles. The porous structure significantly facilitates the transporting of reactant materials and products via the interior space due to the interconnected porous networks and favors the harvesting of light due to enlarged surface area and multiple scattering within the porous network [30]. The specific surface areas of polyaniline-TiO₂/GO and pure TiO₂ are 198.4 and 52.03 m² g⁻¹, respectively. It can be concluded that the hybridization of TiO₂ with polyaniline may significantly enhance its surface area. Polyaniline prevents particle growth during drying step because of mixed bond Ti\O\C, which can prevent the interaction among Ti particles. Beside the effect on the surface area of the nanocomposite, BET characterization implies that hybridization of TiO₂ with polyaniline enhances its pore volume. Particularly, it reaches 0.291 cm³ g⁻¹ for polyaniline-TiO₂/GO composite, which is higher than 0.291 cm³ g⁻¹ of pure TiO₂ (it is not shown for TiO₂). It is accepted in heterogeneous photocatalysis process, higher surface area and pore volume are helpful in the formation of photogenerated $e^- - h^+$ pairs. Therefore, heterogeneous photocatalysis is affected greatly via the surface area and pore structure [31].

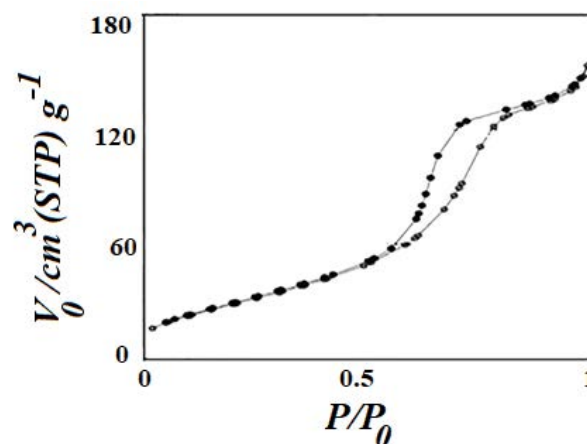


Fig. 6. N₂ adsorption–desorption isotherms of polyaniline-TiO₂/GO nanocomposite.

3.2. Photocatalytic removal of methyl orange using synthesized samples

Langmuir–Hinshelwood (L–H) kinetic model is the most commonly used kinetic expression to describe the photocatalytic removal of organic pollutants from aqueous solutions [32]. The L–H kinetic equation is represented via Eq. 4:

$$\ln \frac{C_0}{C_t} = k_{ap} t \quad (4)$$

where C_0 (mg L⁻¹) and C_t (mg L⁻¹) are the concentration of methyl orange at 0 and t min, respectively. The apparent rate constant, k_{ap} (min⁻¹), can be resulted from the slope of the $\ln \frac{C_0}{C_t}$ vs. time plot. The pseudo-first-order reaction rate constant (k_{ap}) is selected as the basic kinetic factor to compare the photocatalytic activity of synthesized samples. The results of removal of methyl orange using prepared samples under black light illumination are presented in Fig. 7. It could be seen that photocatalytic activity of TiO₂/GO catalyst is higher than that of TiO₂. Therefore, interactions between graphene and TiO₂ lead to the improvement of the photocatalytic activity. The high photocatalytic activity of TiO₂/GO catalyst is because of the following several parameters:

- CB position of TiO₂ is calculated to be 3 eV, and the work function of graphene is about 4.42 eV. So, graphene can act as acceptor positions for photo-generated electrons from TiO₂. Under excitation, the CB electrons of TiO₂ are transferred to graphene. Therefore, the recombination of photo-generated electron–hole pairs can be inhibited [33]. So, the improvement in photocatalytic activity of TiO₂/GO is imaginable.
- The electrons on the graphene can be trapped via oxygen and water on the surface of TiO₂/GO catalyst and generate the hydroxyl and superoxide radicals. As a result, electron–hole recombination is largely prevented and this further facilitates the formation of more OH• because of the valence band of TiO₂ and the superoxide radicals anion (O₂^{•-}) at the surface of catalyst, which in turn results in a faster removal of methyl orange [34].

From Fig. 7, photocatalytic activity of polyaniline-TiO₂/GO is considerably higher than that of TiO₂/GO.

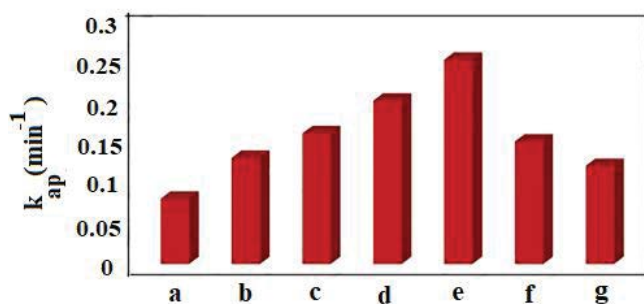
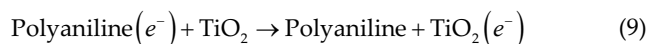
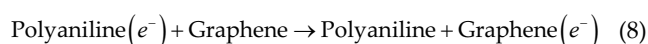
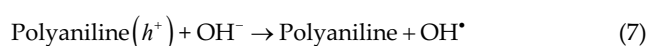
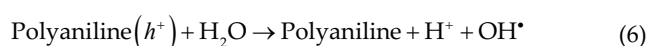
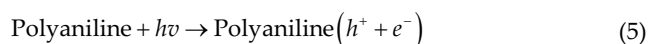


Fig. 7. Photocatalytic removal of methyl orange in the presence of (a) TiO₂, (b) TiO₂/GO, (c) 3 polyaniline-TiO₂/GO, (d) 5 polyaniline-TiO₂/GO, (e) 10 polyaniline-TiO₂/GO, (f) 15 polyaniline-TiO₂/GO and (g) 20 polyaniline-TiO₂/GO.

The photocatalytic removal of methyl orange can take place through a series of reactions on the surface of the samples, such as (i) interaction of methyl orange with polyaniline-TiO₂/GO nanocomposite, (ii) intermediate products (photocatalysis), (iii) colorless degradation product and (iv) saturation of polyaniline-TiO₂/GO nanocomposite surface [34]. Polyaniline acts as a photosensitizer in polyaniline-TiO₂/GO to sensitize the TiO₂ surface. The conduction position of TiO₂ was lower than the lowest unoccupied molecular orbital (LUMO) of polyaniline. The CB of TiO₂ can act as a sink for photogenerated electrons in the hybrid photocatalyst. Under black-light illumination, π – π transition occurred in polyaniline and electrons with highest occupied molecular orbital (HOMO) become excited and transfer to the LUMO of polyaniline. These electrons from the LUMO level are injected into the CB of TiO₂, which react with molecular oxygen and produce O₂^{•-} and HO₂[•] in the aqueous solution [19,35]. Graphene nanosheets are well-known electron acceptor materials which applied widely for decreasing the band gap of TiO₂ to make it active in visible region via the energetically favored hybridization of C_{2p} and O_{2p} atoms of graphene and TiO₂ [36,37]. So, the electrons from the CB of TiO₂ and the LUMO of polyaniline may also be transferred to graphene. The electrons on the graphene can be trapped via oxygen and water on the surface of polyaniline-TiO₂/GO and generate the hydroxyl and superoxide radicals [38,39]. Furthermore, photogenerated holes in the HOMO level of polyaniline also produce hydroxyl radicals upon light excitation [40,41].



Furthermore, in polyaniline-TiO₂/GO catalysts, the polyaniline content can play a significant role in affecting photocatalytic activity of photocatalysts. The results of

removal of methyl orange using polyaniline-TiO₂/GO catalysts with different polyaniline contents (3 polyaniline-TiO₂/GO, 5 polyaniline-TiO₂/GO, 10 polyaniline-TiO₂/GO, 15 polyaniline-TiO₂/GO and 20 polyaniline-TiO₂/GO) are illustrated in Fig. 7. From 3 polyaniline-TiO₂/GO to 10 polyaniline-TiO₂/GO, the photocatalytic activity was gradually increased, and 10 polyaniline-TiO₂/GO showed the maximized photoactivity. However, when the content of polyaniline is further enhanced above its optimum value, the photocatalytic performance deteriorates. The high photoactivity of 10 polyaniline-TiO₂/GO can be described as following reasons:

- The presence of imperfections may omit the polyaniline chain stretching procedure [35], which decreases polyaniline conductivity.
- Because of high aniline concentrations, oxidation products with amino groups in the ortho-position (i.e., imperfections) can be produced, which may alert the polyaniline chain structure and consequently polymer-pollutant interactions [36].

3.3. Adsorptive removal of methyl orange using synthesized samples

Fig. 8 shows the adsorptive removal of methyl orange from aqueous solution using polyaniline-TiO₂/GO and TiO₂/GO samples. Results showed that efficiency of methyl orange removal in the presence of polyaniline-TiO₂/GO is higher. Accumulation of a substance between the liquid–solid interface or gas–solid interface because of physical or chemical associations is termed an adsorption procedure. Adsorption process can be controlled via physical parameters on most of the adsorbents such as polarity, Van der Waals forces, hydrogen bonding, dipole–dipole interaction, π – π interaction, etc. [37]. So, the design of an adsorbent generally depends on the type of substance to be adsorbed or removed. Methyl orange is an anionic dye that can be removed by an adsorbent showing strong affinity toward negatively-charged species. Polyaniline in its conductive emeraldine salt state possesses a large number of amine (–N<) and imine (–N=) functional groups and substantial amounts of positive charges localized over its backbone, making it an efficient candidate for the adsorption of negatively polarized materials. This electrostatic force of attraction could be the essential driving force leading to the increased adsorption of methyl orange.

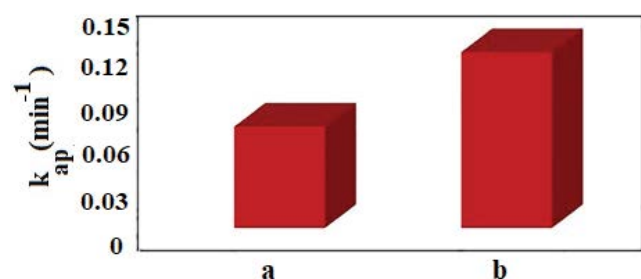


Fig. 8. Adsorptive removal of methyl orange from aqueous solution in the presence of (a) TiO₂/GO and (b) polyaniline-TiO₂/GO samples.

So, the presence of polyaniline in synthesized nanocomposite plays a crucial role in the removal of anionic dye from aqueous solutions [38].

3.4. Effect of contact time

The adsorption kinetics of methyl orange onto polyaniline-TiO₂/GO nanocomposite was studied for 60 min contact time and the results are illustrated in Fig. 9. Within exposure time of 60 min, the adsorbed methyl orange via polyaniline-TiO₂/GO nanocomposite reached to 44.3 mg g⁻¹. The removal of methyl orange by adsorption onto polyaniline-TiO₂/GO nanocomposite was very fast during the initial contact time and then slowed down. This behavior could be related to the availability of a large number of vacant surface sites during the initial stage of adsorption procedure. However, with passage of time, the remaining vacant surface sites are difficult to be occupied because of repulsive forces between the solute molecules on the solid phase and in the bulk liquid phase [39].

The results indicated that the removal rate of methyl orange via polyaniline-TiO₂/GO nanocomposite under photocatalytic procedure was considerably higher than the adsorption procedure, implying that the synergistic adsorption-photocatalysis had definitely occurred. This observation clearly showed that during the removal of methyl orange via polyaniline-TiO₂/GO nanocomposite under light illumination, both adsorption and photocatalytic procedures occurred simultaneously. During the experiment in the dark, the rate of removal of methyl orange by the adsorption procedure was calculated to be 0.116 min⁻¹. However, when polyaniline-TiO₂/GO nanocomposite was exposed to light illumination, the rate of removal of methyl orange jumped to 0.253 min⁻¹ implying that both photocatalytic and adsorption procedures manifested simultaneously.

3.5. Adsorption isotherm studies

The isotherm study was performed to investigate the efficiency of the adsorbent for full-scale applications and design purposes. Langmuir and Freundlich models as the most widely used isotherm models were investigated. The linear form of the Langmuir model is shown via Eq. 14:

$$\frac{1}{q_e} = \left(\frac{1}{k_t q_m} \right) \frac{1}{C_e} + \frac{1}{q_m} \quad (14)$$

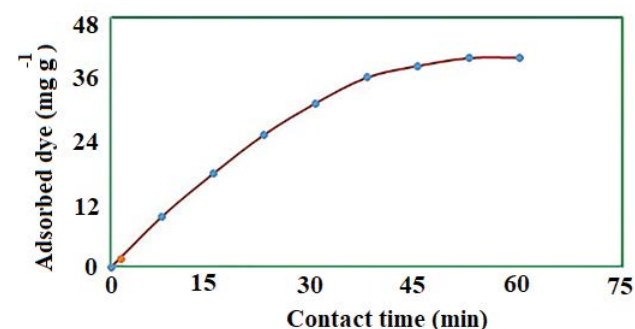


Fig. 9. Effect of contact time on methyl orange adsorption onto polyaniline-TiO₂/GO nanocomposite.

where C_e (mg L^{-1}), q_e (mg g^{-1}), q_m (mg g^{-1}) and K_L (L mg^{-1}) are the equilibrium concentration of methyl orange, the amount of methyl orange adsorbed at equilibrium, the maximum amount of adsorbed pollutant per unit weight of the adsorbent, and the affinity of the binding sites (Langmuir constant), respectively. The linear form of the Freundlich isotherm model is shown via Eq. 15:

$$\ln q_e = \frac{1}{n} \ln C_e + \ln K_F \quad (15)$$

where n and K_F [$(\text{mg g}^{-1}) (\text{L mg}^{-1})^{1/n}$] are the constants related to the adsorption intensity and adsorption capacity, respectively. The values of Langmuir and Freundlich parameters can be estimated from the slope and intercept of linear plots of $1/q_e$ vs. $1/C_e$ and $\ln q_e$ vs. $\ln C_e$, respectively. Fig. 10 illustrates the adsorption isotherms plots. From the slopes and intercepts, the values of q_m , K_L , n and K_F were calculated and represented in Table 1. It can be observed from Table 1, the obtained correlation coefficient for Langmuir model was higher than that of Freundlich model, which implies the suitability of Langmuir isotherm model for describing adsorption of methyl orange onto polyaniline-TiO₂/GO nanocomposite. Based on Langmuir model, the maximum adsorption capacity of polyaniline-TiO₂/GO nanocomposite for the adsorption of methyl orange was found to be 69.23 mg g^{-1} . Essential features of Langmuir isotherm model can be expressed in term of separation factor, R_L , as represented through Eq. 16:

$$R_L = \frac{1}{1 + K_L C_0} \quad (16)$$

where C_0 (mg L^{-1}) is the initial pollutant concentration [40]. The values of R_L arranged as $R_L = 0$, $0 < R_L < 1$ and $R_L > 1$ indicate that adsorption process is irreversible, favorable and unfavorable, respectively. Table 1 demonstrates that R_L values are between 0.282 and 0.86, which implies the adsorption of methyl orange onto polyaniline-TiO₂/GO nanocomposite is favorable [41].

3.6. Thermodynamic study

The thermodynamic study was performed to reach a better understanding of the adsorptive behavior of methyl orange toward polyaniline-TiO₂/GO nanocomposite. This part of

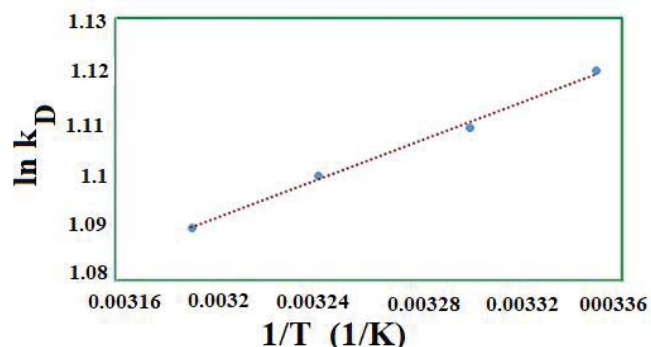


Fig. 10. Thermodynamic profile for methyl orange adsorption onto polyaniline-TiO₂/GO nanocomposite.

Table 1
Isotherm parameters for methyl orange adsorption onto polyaniline-TiO₂/GO nanocomposite

Type of isotherm model	Value
Langmuir isotherm	
q_m (mg g^{-1})	69.23
K_L (L mg^{-1})	0.127
R_L	0.282–0.86
R^2	0.9925
Freundlich isotherm	
K_F (mg g^{-1})	4.055
N	1.43
R^2	0.9823

experiments was carried out by varying the temperature between 25°C and 40°C (298–313 K). The free energy change or Gibbs free energy (ΔG°) (kJ mol^{-1}), enthalpy change (ΔH°) (kJ mol^{-1}) and entropy change (ΔS°) ($\text{kJ mol}^{-1} \text{ K}^{-1}$) for the adsorption of methyl orange were calculated through Eqs. 17 and 18:

$$\Delta G^\circ = -RT \ln K_D \quad (17)$$

$$\ln K_D = \left(\frac{\Delta S^\circ}{R} \right) - \left(\frac{\Delta H^\circ}{RT} \right) \quad (18)$$

where R , T (K) and K_D (q_e/C_e) are the universal gas constant, temperature and the distribution coefficient, respectively [55]. To study the thermodynamic of methyl orange adsorption onto polyaniline-TiO₂/GO nanocomposite, thermodynamic constants such as ΔG° , ΔH° and ΔS° were calculated using Eqs. 17 and 18. From the slope ($-\Delta H^\circ/R$) and intercept ($\Delta S^\circ/R$) of the plot of $\ln K_D$ versus $1/T$, the ΔH° and ΔS° of adsorption were estimated, respectively (Fig. 10). The values of these parameters are summarized in Table 2. As exhibited, the negative ΔH° and ΔG° values demonstrated that the adsorption of methyl orange onto polyaniline-TiO₂/GO nanocomposite was exothermic and spontaneous in nature, respectively. The negative value of ΔS° indicates the decrease of degree of freedom of adsorbed pollutant on the binding sites of the nanocomposite at the solid–solution interface, implying a strong binding of dye ions onto the active sites [42].

Table 2
Obtained parameters from thermodynamic study of methyl orange adsorption onto polyaniline-TiO₂/GO nanocomposite

Temperature (K)	ΔG° (kJ mol^{-1})	ΔS° ($\text{kJ mol}^{-1} \text{ K}^{-1}$)	ΔH° (kJ mol^{-1})
298	-2.85	-0.0027	-2.97
303	-2.82	-	-
308	-2.74	-	-
313	-2.77	-	-

4. Conclusions

The present work was carried out to synthesize and investigate the efficiency of polyaniline-TiO₂/GO nanocomposite to adsorb and degrade an anionic dye (methyl orange) from aqueous solution. SEM analysis proved a highly porous structure for polyaniline-TiO₂/GO nanocomposite, which is suitable for sequestering dye molecules in aqueous phase. The average size of the primary particles estimated from the TEM image was about 8–10 nm. DRS study showed that polyaniline-TiO₂/GO nanocomposite possessed a much lower recombination rate of charge carriers and higher black light activity. Among various isotherm models, the Langmuir isotherm showed the best fit to experimental data. The separation factor, R_L , was obtained less than 1, indicating the favorable nature of methyl orange adsorption on polyaniline-TiO₂/GO nanocomposite. Besides, the results of thermodynamic investigation showed that the adsorption of methyl orange via polyaniline-TiO₂/GO nanocomposite is spontaneous and exothermic.

Acknowledgment

We express our gratitude to the Payame Noor University for supporting this project.

References

- [1] Y. Jin, Y. Wu, J. Cao, Optimizing decolorization of Methylene Blue and Methyl Orange dye by pulsed discharged plasma in water using response surface methodology, *J. Taiwan Inst. Chem. Eng.*, 45 (2014) 589–595.
- [2] D.I. Çifçi, Decolorization of methylene blue and methyl orange with Ag doped TiO₂ under UV-A and UV-visible conditions: process optimization by response surface method and toxicity evaluation, *Global NEST J.*, 18 (2016) 371–380.
- [3] P. Deka, A. Hazarika, R.C. Deka, P. Bharali, Influence of CuO morphology on the enhanced catalytic degradation of methylene blue and methyl orange, *RSC Adv.*, 6 (2016) 95292–95305.
- [4] S. Mortazavi-Derazkola, M. Salavati-Niasari, O. Amiri, A. Abbasi, Fabrication and characterization of Fe₃O₄@SiO₂@TiO₂@Ho nanostructures as a novel and highly efficient photocatalyst for degradation of organic pollution, *J. Energy Chem.*, 26 (2017) 17–23.
- [5] H. Eskandarloo, A. Badiie, M.A. Behnajady, Optimization of UV/inorganic oxidants system efficiency for photooxidative removal of an azo textile dye, *Desal. Wat. Treat.*, 55 (2015) 210–226.
- [6] V. Altun, J.C. Remigy, I.F.J. Vankelecom, UV-cured polysulfone-based membranes: effect of co-solvent addition and evaporation process on membrane morphology and SRNF performance, *J. Membr. Sci.*, 524 (2017) 729–737.
- [7] C. Emin, Y. Gu, J.C. Remigy, J.F. Lahitte, Polyethersulfone hollow fiber modified with poly (styrenesulfonate) and Pd nanoparticles for catalytic reaction, *Eur. Phys. J. Spec. Top.*, 224 (2015) 1843–1848.
- [8] M. Tanzifi, M. Mansouri, M. Heidarzadeh, K. Gheibi, Study of the adsorption of Amido Black 10B dye from aqueous solution using polyaniline nano-adsorbent: kinetic and isotherm studies, *J. Water Environ. Nanotechnol.*, 1 (2016) 124–134.
- [9] S. Shahabuddin, N.M. Sarih, M.A. Kamboh, H.R. Nodeh, S. Mohamad, Synthesis of polyaniline-coated graphene oxide@SrTiO₃ nanocube nanocomposites for enhanced removal of carcinogenic dyes from aqueous solution, *Polymers*, 8 (2016) 305.
- [10] R. Mohammadi, B. Massoumia, B. Emamalinassaba, H. Eskandarloo, Cu-doped TiO₂-graphene/alginate nanocomposite for adsorption and photocatalytic degradation of methylene blue from aqueous solutions, *Desal. Wat. Treat.*, 82 (2017) 81–91.
- [11] M.K.M. Nodeh, S. Soltani, S. Shahabuddin, H.R. Nodeh, H. Sereshti, Equilibrium, kinetic and thermodynamic study of magnetic polyaniline/graphene oxide based nanocomposites for Ciprofloxacin removal from water, *J. Inorg. Organomet. Polym. Mater.*, 28 (2018) 1226–1234.
- [12] A.M. Golsheikh, H.N. Lim, R. Zakaria, N.M. Huang, Sonochemical synthesis of reduced graphene oxide uniformly decorated with hierarchical ZnO nanospheres and its enhanced photocatalytic activities, *RSC Adv.*, 5 (2015) 12726–12735.
- [13] S.N.A. Baharin, N.M. Sarih, S. Mohamad, S. Shahabuddin, K. Sulaiman, A. Ma'amor, Removal of endocrine disruptor di-(2-ethylhexyl)phthalate by modified polythiophene-coated magnetic nanoparticles: characterization, adsorption isotherm, kinetic study, thermodynamics, *RSC Adv.*, 6 (2016) 44655–44667.
- [14] R.D.C. Soltani, A.R. Khataee, M. Safari, S.W. Joo, Preparation of bio-silica/chitosan nanocomposite for adsorption of a textile dye in aqueous solutions, *Int. Biodeterior. Biodegradation*, 85 (2013) 383–391.
- [15] H. Eskandarloo, A. Badiie, Fabrication of an inexpensive and high efficiency microphotoreactor using CO₂ laser technique for photocatalytic water treatment applications, *Environ. Technol.*, 36 (2015) 1063–1073.
- [16] X. Zhang, M.Z. Yates, Enhanced photocatalytic activity of TiO₂ nanoparticles supported on electrically polarized hydroxyapatite, *ACS Appl. Mater. Interfaces*, 10 (2018) 17232–17239.
- [17] K. Nakata, A. Fujishima, TiO₂ photocatalysis: design and applications, *J. Photochem. Photobiol., C*, 13 (2012) 169–189.
- [18] F. Zhang, H. Cao, D. Yue, J. Zhang, M. Qu, Enhanced anode performances of polyaniline-TiO₂-reduced graphene oxide nanocomposites for lithium ion batteries, *Inorg. Chem.*, 51 (2012) 9544–9551.
- [19] K. Shetty, B.S. Prathibha, D. Rangappa, K.S. Anantharaju, H.P. Nagaswarupa, H. Nagabhushana, S.C. Prashantha, Photocatalytic study for fabricated Ag doped and undoped MgFe₂O₄ nanoparticles, *Mater. Today: Proc.*, 4 (2017) 11764–11772.
- [20] D.P. Kumar, N.L. Reddy, B. Srinivas, V.D. Kumari, M.V. Shankar, Influence of reaction parameters for the enhanced photocatalytic hydrogen production using surface modified semiconductor titania nanotubes, *Mater. Today: Proc.*, 4 (2017) 11653–11659.
- [21] K. Sakurai, M. Mizusawa, X-ray diffraction imaging of anatase and rutile, *Anal. Chem.*, 82 (2010) 3519–3522.
- [22] T.C. Wen, Y.S. Li, K. Rajamani, H.J. Harn, S.Z. Lin, T.W. Chiou, Effect of Cinnamomum osmophloeum Kanehira leaf aqueous extract on dermal papilla cell proliferation and hair growth, *Cell Transplant.*, 27 (2018) 256–263.
- [23] M. Hojamberdiev, G. Zhu, A. Eminov, K. Okada, Template-free hydrothermal synthesis of hollow α -FeOOH urchin-like spheres and their conversion to α -Fe₂O₃ under low-temperature thermal treatment in air, *J. Cluster Sci.*, 24 (2013) 97–106.
- [24] H. Eskandarloo, M. Zaferani, A. Kierulf, A. Abbaspourrad, Shape-controlled fabrication of TiO₂ hollow shells toward photocatalytic application, *Appl. Catal. B*, 227 (2018) 519–529.
- [25] S. Cingarapu, M.A. Ikenberry, D.B. Hamal, C.M. Sorensen, K. Hohn, K.J. Klabunde, Transformation of indium nanoparticles to β -indium sulfide: digestive ripening and visible light-induced photocatalytic properties, *Langmuir*, 28 (2012) 3569–3575.
- [26] A.B. Moghaddam, T. Nazari, J. Badraghi, M. Kazemzad, Synthesis of ZnO nanoparticles and electrodeposition of polypyrrole/ZnO nanocomposite film, *Int. J. Electrochem. Sci.*, 4 (2009) 247–257.
- [27] M.R. Nabid, S. Asadi, R. Sedghi, A.B. Moghaddam, Chemical and enzymatic polymerization of polyaniline/Ag nanocomposites, *Chem. Eng. Technol.*, 36 (2013) 1411–1416.
- [28] M.B. Radoicic, Z.V. Saponjic, M.T. Marinovic-Cincovic, S.P. Ahrenkiel, N.M. Bibic, J.M. Nedeljkovic, The influence of shaped TiO₂ nanofillers on the thermal properties of poly vinyl-alcohol, *J. Serb. Chem. Soc.*, 77 (2012) 699–714.
- [29] M.A. Khan, W.T. Wallace, S.Z. Islam, S. Nagpure, J. Strzalka, J.M. Littleton, S.E. Rankin, B.L. Knutson, Adsorption and recovery of polyphenolic flavonoids using TiO₂-functionalized mesoporous silica nanoparticles, *ACS Appl. Mater. Interfaces*, 9 (2017) 32114–32125.

- [30] P. Modak, S.B. Kondawar, D.V. Nandanwar, Synthesis and characterization of conducting polyaniline/graphene nanocomposites for electromagnetic interference shielding, *Procedia Mater. Sci.*, 10 (2015) 588–594.
- [31] P. Saini, V. Choudhary, B.P. Singh, R.B. Mathur, S.K. Dhavan, Polyaniline–MWCNT nanocomposites for microwave absorption and EMI shielding, *Mater. Chem. Phys.*, 113 (2009) 919–926.
- [32] Y. Li, H. Peng, G. Li, K. Chen, Synthesis and electrochemical performance of sandwich like grapheme-polyaniline composite nanosheets, *Eur. Polym. J.*, 48 (2012) 1406–1412.
- [33] J. Schneider, M. Matsuoka, M. Takeuchi, J. Zhang, Y. Horiuchi, M. Anpo, D.W. Bahnemann, Understanding TiO₂ photocatalysis: mechanisms and materials, *Chem. Rev.*, 114 (2014) 9919–9986.
- [34] Z.F. Li, Jian. Xie, L. Stanciu, Y. Ren, Nano-structured graphenes and metal oxides for fuel cell and battery applications, *Adv. Mater. Res.*, 705 (2013) 126–131.
- [35] A.L. Linsebigler, G. Lu, J.T. Yates, Photocatalysis on TiO₂ surfaces: principles, mechanisms, and selected results, *Chem. Rev.*, 95 (1995) 735–758.
- [36] N. Bao, S. He, Q.Z. Zhang, Z. Yin, Y.X. Zhang, X.H. Xu, Synthesis of dual-phase titanate/anatase with controllable morphology doped with nitrogen from a bola-amphiphile amine surfactant as template, *Ceram. Int.*, 41 (2015) 5916–5925.
- [38] V. Sharma, P. Rekha, P. Mohanty, Nanoporous hypercrosslinked polyaniline: an efficient adsorbent for the adsorptive removal of cationic and anionic dyes, *J. Mol. Liq.*, 222 (2016) 1091–1100.
- [39] H. Eskandarloo, A. Badiei, M.A. Behnajady, Application of response surface methodology for optimization of operational variables in photodegradation of phenazopyridine drug using TiO₂/CeO₂ hybrid nanoparticles, *Desal. Wat. Treat.*, 54 (2015) 3300–3310.
- [40] S.W. Lam, A. Soetanto, R. Amal, Self-cleaning performance of polycarbonate surfaces coated with titania nanoparticles, *J. Nanopart. Res.*, 11 (2009) 1971–1979.
- [41] H. Zhang, R.L. Zong, J.C. Zhao, Y.F. Zhu, Dramatic visible photocatalytic degradation performances due to synergetic effect of TiO₂ with PANI, *Environ. Sci. Technol.*, 42 (2008) 3803–3807.
- [42] S. Singh, P.K. Singh, H. Mahalingam, Novel floating Ag⁺-doped TiO₂/polystyrene photocatalysts for the treatment of dye wastewater, *Ind. Eng. Chem. Res.*, 53 (2014) 16332–16340.